

Optomechanical-organized multipulse dynamics in ultrafast fiber laser

Lin Huang(黄琳), Yu-Sheng Zhang(张裕生), and Yu-Dong Cui(崔玉栋)

Citation: Chin. Phys. B, 2021, 30 (**11**): 114203. DOI: 10.1088/1674-1056/abf344
Journal homepage: http://cpb.iphy.ac.cn; http://iopscience.iop.org/cpb

What follows is a list of articles you may be interested in

Generation of domain-wall solitons in an anomalous dispersion fiber ring laser

Wen-Yan Zhang(张文艳), Kun Yang(杨坤), Li-Jie Geng(耿利杰), Nan-Nan Liu(刘楠楠), Yun-Qi Hao(郝蕴琦), Tian-Hao Xian(贤天浩), and Li Zhan(詹黎)

Chin. Phys. B, 2021, 30 (**11**): 114212. DOI: 10.1088/1674-1056/ac0e22

A low-threshold multiwavelength Brillouin fiber laser with double-frequency spacing based on a small-core fiber

Lu-Lu Xu(徐路路), Ying-Ying Wang(王莹莹), Li Jiang(江丽), Pei-Long Yang(杨佩龙), Lei Zhang(张磊), and Shi-Xun Dai(戴世勋)

Chin. Phys. B, 2021, 30 (**8**): 084210. DOI: 10.1088/1674-1056/abff47

Two-dimensionally controllable DSR generation from dumbbell-shaped mode-locked all-fiber laser

Zhi-Yuan Dou(窦志远), Bin Zhang(张斌), Jun-Hao Cai(蔡君豪), Jing Hou(侯静)

Chin. Phys. B, 2020, 29 (**9**): 094201. DOI: 10.1088/1674-1056/ab9de1

A 3-kHz Er: YAG single-frequency laser with a ‘triple-reflection’ configuration on a piezoelectric actuator

Shuai Huang(黄帅), Qing Wang(王庆), Meng Zhang(张濛), Chaoyong Chen(陈朝勇), Kaixin Wang(王凯鑫), Mingwei Gao(高明伟), Chunqing Gao(高春清)

Chin. Phys. B, 2020, 29 (**8**): 084204. DOI: 10.1088/1674-1056/ab9441

Influences of annealing temperature on properties of Fe^{2+}: ZnSe thin films deposited by electron beam evaporation and their applications to *Q*-switched fiber laser

Du-Xin Qing(卿杜鑫), Shu-Tong Wang(王树同), Shou-Gui Ning(宁守贵), Wei Zhang(张伟), Xiao-Xu Chen(陈晓旭), Hong Zhang(张弘), Guo-Ying Feng(冯国英), Shou-Huan Zhou(周寿桓)

Chin. Phys. B, 2020, 29 (**5**): 054208. DOI: 10.1088/1674-1056/ab81f2

Optomechanical-organized multipulse dynamics in ultrafast fiber laser*

Lin Huang(黄琳)[1,2,3,†], Yu-Sheng Zhang(张裕生)[4], and Yu-Dong Cui(崔玉栋)[5]

[1] *Ceyear Technologies Co., Ltd, Qingdao* 266555, *China*
[2] *Science and Technology on Electronic Test & Measurement Laboratory, Qingdao* 266555, *China*
[3] *School of Information Science and Engineering, Shandong University, Qingdao* 266237, *China*
[4] *Hangzhou Institute of Advanced Studies, Zhejiang Normal University, Hangzhou* 311231, *China*
[5] *State Key Laboratory of Modern Optical Instrumentation, College of Optical Science and Engineering, Zhejiang University, Hangzhou* 310027, *China*

(Received 27 January 2021; revised manuscript received 28 March 2021; accepted manuscript online 30 March 2021)

A novel organized multipulse pattern and its birth dynamics under strong optomechanical effect in microfiber-assisted ultrafast fiber laser are investigated in this work. The background pulses are observed to obviously exhibit selectively amplifying self-organized process of evolving into quasi-stable equidistant clusters. The radio frequency spectrum of the multipulse pattern displays a harmonic mode-locking-like behavior with a repetition rate of 2.0138 GHz, corresponding to the frequency of torsional-radial (TR_{2m}) acoustic mode in microfiber. The results show the evidence of optomechanical effect in dominating the birth dynamics and pattern of multipulse.

Keywords: fiber lasers, multipulse operation, optomechanical effect

PACS: 42.55.Wd, 42.65.–k, 42.81.–i **DOI:** 10.1088/1674-1056/abf344

1. Introduction

Ultrafast fiber laser is becoming the fundamental building block in fields of industry, medicine and scientific research. It also provides an ideal platform for the fundamental research of dissipative soliton characteristics which exhibit profound nonlinear optical dynamics.[1,2] Exploring the nonlinear dynamics of pulse in laser has deepened the understanding of the properties and interactions of solitons. It also offers a powerful tool to manipulate the operation states of lasers.

Among these researches, multipulse dynamics at elevated pump power has attracted much attention in a wide range of scientific disciplines, due to its rich nonlinear dynamics, abundant operating states and significant potential for practical applications in high speed telecommunication, laser machining, advanced information processing, *etc*. Multipulse operation is a state that multiple ordered or disordered pulses coexist in one roundtrip, such as soliton molecule,[3,4] supramolecular,[5] harmonic mode-locking (HML),[6,7] and soliton rains.[8,9] The formation and stabilization of these states are mediated by the short- and long-range pulse interactions[10] driven by the repulsive and attractive forces induced by coherent overlap,[2] dispersive wave (DW),[11,12] gain depletion and recovery (GDR),[13,14] optomechanical effects,[15,16] noise mediated Casimir-like effects,[8,17] *etc*. Among these effects, the optomechanical effect, as a significant determinant, is the most powerful tool for controlling and realizing the organized multipulse operation.

In mode-locked fiber lasers, the optomechanical effect induces interpulse interaction through optically-driven transverse acoustic wave, including the radial (R_{0m}) and torsional-radial (TR_{2m}) acoustic modes. The electrostrictively excited acoustic wave can periodically perturb the refractive index of the fiber, giving rise to the change of the group velocities and phases of subsequent pulses.[12,18] This R_{0m} induced optomechanical effect has been reported to be involved in compound pattern,[19] and HML.[12,18] The recent studies show that the stabilization of HML is due to the acoustic resonance,[6,15,20] where multiple integer of pulse repetition rates lies in the acoustic gain band. Importantly, the gain and frequency of acoustic wave can be greatly enhanced in tiny core fibers.[21,22] Using enhanced optomechanical effects, the stable HML at a GHz repetition rate have been reported in photonics crystal fibers based fiber lasers.[20] Strong interest in the enhanced optomechanical effects lies in the fact that they are able to generate individual control elements to realize the organized multipulse operations, such as controllable and organized optomechanically bound states of solitons,[15] supramolecular[5] and optical-soliton reactors.[23] The TR_{2m} acoustic wave can induce polarization modulation of the light in optical fiber.[24] The polarization modulation can be transformed into the intensity modulation through polarizer, which can characterize the diameter of fibers[25] and give rise to the modulation peak of continuous wave in nonlinear-polarization-rotation (NPR)

*Project supported by the National Natural Science Foundation of China (Grant Nos. 61525505, 11774310, and 62035010) and the Postdoctoral Science Foundation of China (Grant No. 2019M652076).

†Corresponding author. E-mail: huanglin@ceyear.com

© 2021 Chinese Physical Society and IOP Publishing Ltd

mode-locked fiber lasers.[26] Although the gain of the TR_{2m} is generally lower than that of R_{0m} acoustic mode, the recent experimental results have demonstrated the ability to stabilize the HML by the TR_{2m} acoustic resonance.[27] We have also demonstrated that the GHz HML can be predominately stabilized by the TR_{21} rather than R_{01} acoustic resonance in microfiber-assisted ultrafast fiber laser.[28] In microfiber, the enhanced optomechanical effect induced by TR_{2m} acoustic mode can possibly dominate the pulse interaction that is hindered for that of R_{0m} and in conventional fibers due to the weak optomechanical effect and the competing pulse interacting mechanisms.

By using the enhanced TR_{21} induced optomechanical effect, in this work, we report the real-time observation of a novel organized multipulse pattern and its self-organized buildup dynamics in microfiber-assisted ultrafast fiber laser. Under strong optomechanical effect induced by TR_{21} acoustic mode supported by the microfiber, the multiple background pulses can be selectively amplified into multiple clusters; the clusters are locked by the evenly spaced lattices induced by the optomechanical effect. In addition, the radio-frequency (RF) spectrum shows HML-like behavior at a repetition rate of 2.0138 GHz, with good stability and high side mode suppression ratio.

2. Experimental details

The experimental setup of the microfiber-assisted NPR mode-locked fiber laser is shown in Fig. 1. The system consists of two wavelength division multiplexers (WDM, 980 nm/1550 nm), 8-m-long EDF (Nufern EDFC-980-HP) with 6-dB/m peak core absorption pumped by two laser diodes (LD): one is the polarization sensitive isolator sandwiched between two polarization controllers that constitute an NPR, and the other is optical coupler (OC, 10/90). A microfiber with a total length of $\sim$ 33 cm, waist length of $\sim$ 16 cm and waist diameter estimated as 1.39 μm is adopted to induce the strong optomechanical effect. The microfiber is prepared based on a two-stage flame-brush method,[29,30] and the same method and preparation parameters are described in detail in Ref. [28].

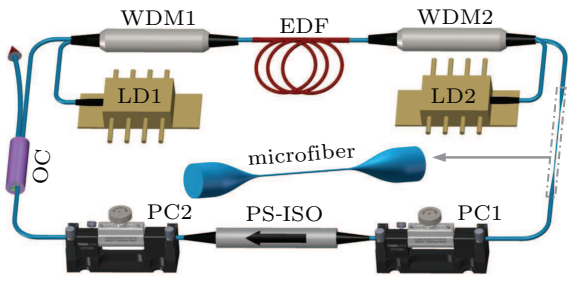


Fig. 1. Schematic diagram of experimental setup for microfiber-assisted ultrafast fiber laser. WDM: wavelength division multiplexer; EDF: erbium-doped fiber; LD: laser diode; PC: polarization controller; PS-ISO: polarization-sensitive isolator; OC: optical coupler.

Considering the enhancement of optomechanical effect in microfier,[31] the $\sim$ 16-cm-long-waist can provide an enough acoustic gain that is comparable to and even larger than that of the SMF in the cavity. The total length of the cavity is $\sim$ 29.2 m, corresponding to the cavity roundtrip time of 143.01 ns, and a fundamental repetition rate of 6.99 MHz. At the output port, real-time temporal detections are recorded with a high-speed real-time oscilloscope (OSC, 16-GHz bandwidth) together with a 16-GHz bandwidth photodetector (PD), the time-averaged spectrum is measured with an optical spectrum analyzer (OSA), and the radio frequency spectrum is recorded with an electrical spectrum analyzer (ESA).

3. Results and discussion

The microfiber-assisted mode-locked laser operates at the continuous-wave at the pump power of $\sim$ 10 mW. With properly tuning the two PCs, the optomechanical-organized equidistant clusters can be rapidly achieved at the pump power higher than 300 mW, with good self-starting ability, repeatability and PC tolerance. The experimental real-time characterization of the buildup process is shown in Fig. 2. The recorded time series is segmented into the roundtrip time (y axis) and roundtrip number (x axis). To show a clearer buildup process, only 5-ns temporal range of one roundtrip time is exhibited. The results in Fig. 2 demonstrate an interesting organized multipulse pattern and buildup process, the entire buildup process includes the relaxation oscillation (RO), the transient self-organization stage and the final equidistant clusters. The entire buildup process takes generally less than 3 ms, and it is

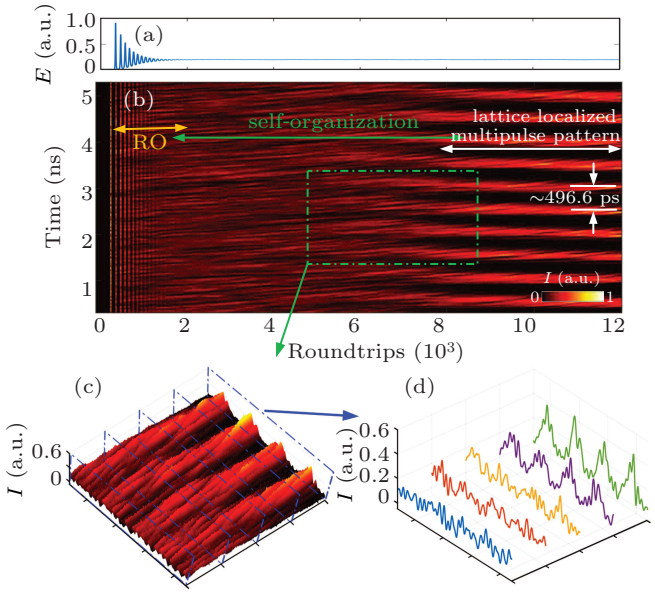


Fig. 2. Experimental real-time characterizations of buildup process of optomechanical-organized multipulse pattern, showing (a) intracavity energy evolution in buildup process, (b) entire buildup process, see visualization 1 for full animation. Note that only 5-ns time range of one roundtrip time is exhibited to show a clear buildup process, (c) close up of self-organization, (d) temporal profile of the pulses at selected roundtrips in panel (c), where RO, I, and E denote relaxation oscillation, intensity, and energy. The abbreviation (a.u.) is short for arbitrary units.

$\sim$ 1.3 ms here. As shown in Fig. 2(a), the RO has a damped behavior and decayed period between adjacent laser spikes, which are the typical characteristics in lasers.[32] The damped RO route is different from the raised RO route[3,33] and the Q-switched route[34] in carbon nanotube mode-locked fiber laser. After the damped RO, the laser evolves into the transient self-organization stage with a duration of $\sim$ 0.9 ms, the close-up is shown in Fig. 2(c). At the beginning of this stage, multiple background pulses (more than one thousand) coexist in each roundtrip, no Q-switched instability can be seen. These pulses experience complex and traceable evolution under the effect of modulation instability, saturable absorbing, gain competition, *etc*. However, at the end of this stage, part of the pulses fades into weaker background pulses, and the remaining pulses display synchronously self-organized process of growing into 288 evenly spaced clusters, showing a selectively amplifying process. However, the intracavity energy remains stable in this self-organizing buildup process as shown in Fig. 2(a). The clusters are quasi-stable, with the spacing between adjacent clusters being $\sim$ 496.6 ps. In each cluster, there are 2–4 pulses at the same time with different intensities and complex evolution dynamics. The temporal profile of the pulses in Fig. 2(c) with 1000-roundtrip interval is shown in Fig. 2(d). It shows that the weak background pulses are amplified inside the equidistant clusters, but suppressed outside the clusters. Note that the birth dynamics here is different from that of HML in all-single-mode-fiber lasers[12,18] and in this cavity that we have studied, the birth dynamics usually originates from the separating process of closely spaced multiple pulses with a duration being on the order of a few seconds.

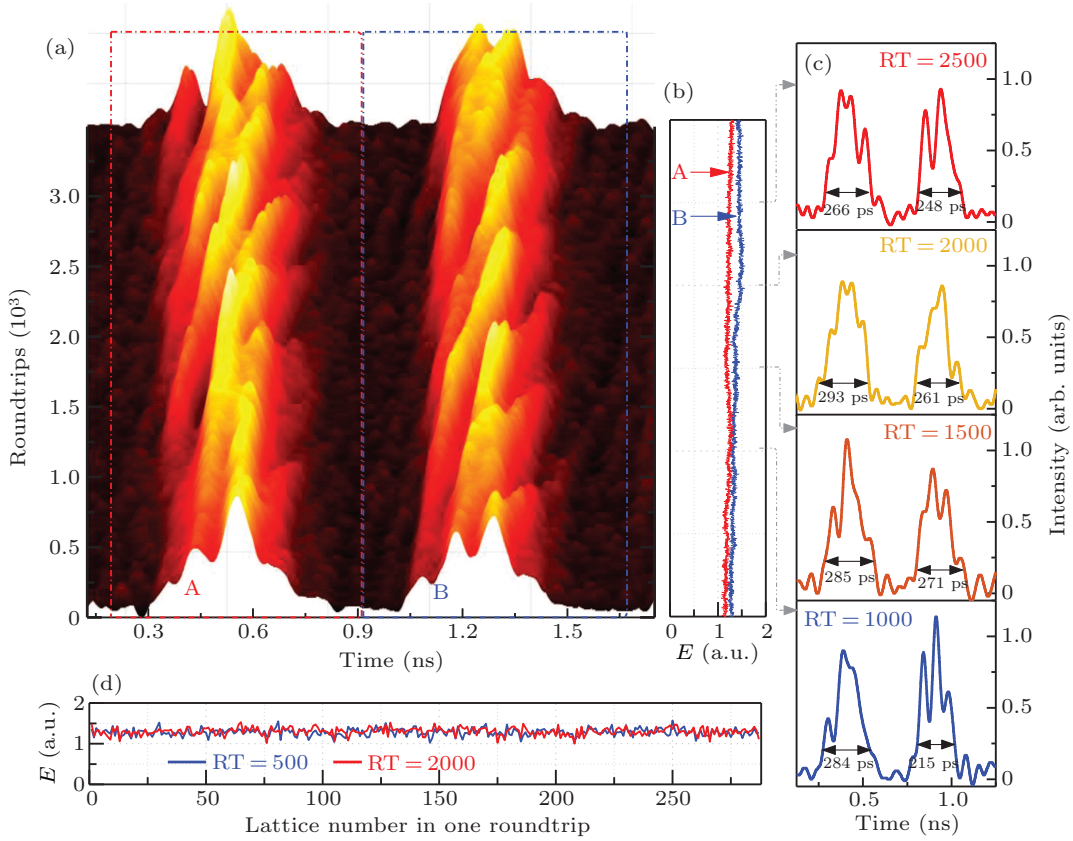


Fig. 3. Dynamics of quasi-steady lattice-localized multipulse pattern, showing (a) consecutive evolution over 3000 roundtrips after $\sim$ 5 min of the onset process, (b) evolution of energy in sections A and B in panel (a), (c) temporal profile of pulses at roundtrips 1000, 1500, 2000, 2500, respectively. Note that only 1-ns time range of one roundtrip time is exhibited here (see Visualization 2 for full animation), and (d) energy distribution in 288 clusters in one roundtrip, where blue and red curves represent roundtrips 500 and 2000, respectively, and RT denotes roundtrip.

The evenly spaced clusters remain quasi-stable and can last for hours even under slight perturbation. The real time evolution of the quasi-stable organized multipulse pattern is recorded by using the OSC with 250-fs time interval. As shown in Fig. 3(a), the result is measured after $\sim$ 5 min of the buildup process. Here only 2 among the 288 clusters in one roundtrip are exhibited. In this quasi-steady state, the spacing between the adjacent clusters keeps constant at $\sim$ 496.6 ps. Although the clusters are stable, the internal dynamics of clusters is complex. Firstly, evolution paths between the clusters and the internal pulses are different, which indicates their group velocities are different from each other. More specifically, the results in Figs. 2(b) and 3(a) show that the cluster internal pulses originate from the weak background pulses. Owing to the velocity difference, the weak background pulses quasi-periodically run into and escape from the cluster, showing a quasi-periodical behavior. Secondly, as shown in Figs. 3(a) and 3(c), the internal pulses are strong in the center

of the cluster but weak at the edge of the cluster. This result indicates that the cluster acts as intensity modulator, pulses in the center of the cluster are amplified most greatly. Meanwhile, as shown in Figs. 3(b) and 3(d), in the 3000 consecutive roundtrips of the 2 clusters, and 288 clusters in roundtrips 500 and 2000, the energy values in the lattices are almost at the same level with slight fluctuations. In addition, as shown in Fig. 3(c), the 7-dB width of the clusters are around 260 ± 40 ps.

Under the quasi-stable state, the 3-dB spectral width of the output spectrum is usually 0.7 nm–1.1 nm, depending on the pump power and the orientations of the PCs. As shown in Fig. 4(a) (blue curve), the spectrum of the quasi-stable multipulse pattern is centered at 1560.34 nm with a 3-dB width of 0.87 nm, which can be considered as a quasi-mode-locking condition. The coexistence of the cluster and the weak background pulses in Fig. 2 also indicates a quasi-mode-locking condition. However, as shown in Figs. 4(b) and 4(c), the RF spectrum show that the quasi-stable multipulse pattern has HML-like character with a stable repetition rate of 2.0138 GHz, which is the 288-th harmonic of the fundamental cavity repetition rate (6.99 MHz). This result is in accordance with the $\sim$ 496.6-ps cluster spacing in Fig. 3. Although obvious side mode can be seen, the side- mode suppression ratio is as high as -38.77 dB at a resolution bandwidth of 4.3 kHz, the signal-to-noise ratio is 42.50 dB at a resolution bandwidth of 9.1 Hz. The 10-GHz span in the inset of Fig. 4(b) shows that the high order harmonic decays with frequency increasing, showing a non-perfect HML operation due to the complex dynamics of the pulses in the clusters.

Owing to the HML-like behavior of the organized equidistant clusters, we believe that this quasi-steady operation and selectively amplifying self-organizing birth dynamics are directly related to the strong optomechanical effect supported by the microfiber. In our previous work, we demonstrated the stable HML in microfiber-assisted ultrafast laser, the GHz repetition rates can be locked to the frequency of R_{01} acoustics mode, and predominantly to that of TR_{21} acoustic mode.[28] In fact, using the same cavity as that shown in Fig. 1, we also obtain HML that is predominately locked at a repetition rate of 2.0068 GHz with typical conventional soliton spectrum (3-dB spectral width is 5.09 nm) as shown in Figs. 4(a) and 4(b) (red curves), HML at a higher repetition rate has also been observed. The results evidence that the stable HML state is due to the TR_{21} acoustic resonance. Thus, the waist diameter of the microfiber is estimated at $\sim$ 1.39 μm by the finite element method.[6] The perfectly matched repetition rate between the real HML and the organized multipulse pattern shows the evidence of the optomechanical effect in stabilizing the lattice-localized multipulse pattern. In fact, the width of the cluster is also in accordance with the impulse response of the acoustic wave, considering only the TR_{21} acoustic mode in the microfiber.[16,35] Note that the 6.99-MHz frequency offset, which corresponds to the cavity fundamental repetition rate, is due to the non-perfect uniform waist diameter of the microfiber and the relatively large intrinsic gain bandwidth of the acoustic wave. This effect has been used to achieve repetition rate tuning in PCF-assisted ultrafast fiber laser.[36] In fact, by replacing the microfiber, we also obtain the organized multipulse pattern with repetition rate depending on the waist diameter of the microfiber.

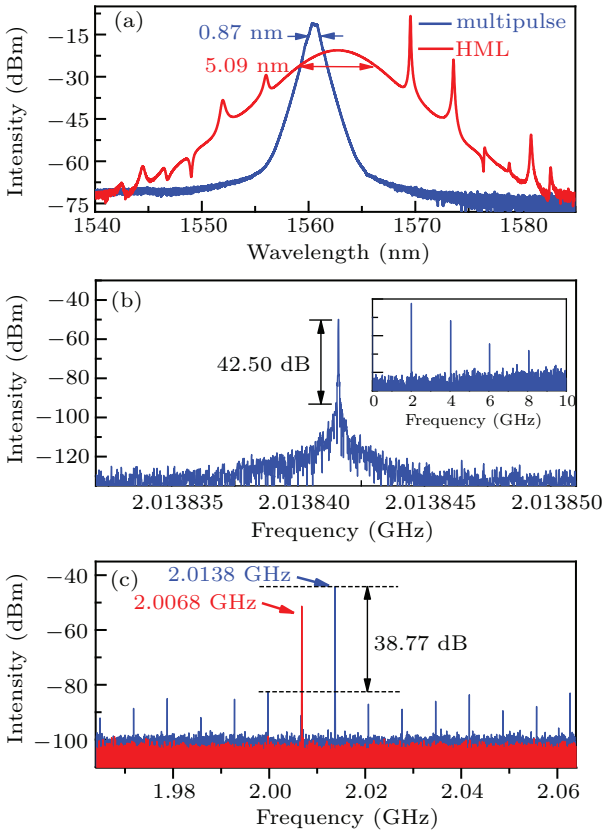


Fig. 4. Experimental results of quasi-steady lattice-localized multipulse pattern: (a) optical spectra; (b) RF spectrum in steps of 2 kHz, with inset showing RF spectrum in steps of 10 GHz; (c) RF spectra of multipulse pattern and HML in steps of 100-MHz span, where blue and red curves represent the results of the optomechanical-organized equidistant clusters and HML operation, respectively. The two results are obtained with the same cavity but different polarization orientations of PCs.

Manifold interaction mechanisms may be involved in the synchronous self-organization stage as shown in Figs. 2(b) and 2(c), such as the saturable absorption and gain competition, a more detailed study is needed to fully explain this process. Nevertheless, we believe that the selective amplifying of the pulses in the self-organization process constituites a general feature of the optomechanical effect. As proved in Ref. [26], the TR_{2m} acoustic response induces polarization modulation which can be transformed into the intensity modulation through the NPR mode-locker, *i.e.*, the optomechanical lattices of the TR_{2m} acoustic vibration act as an intensity modulator in NPR-based mode-locked fiber lasers. In the self-organization process, a relatively large pulses excites the TR_{21} acoustic response, which induces the equidistant optomechan-

ical lattices. Under certain polarizations conditions, pulses run into the lattices are amplified but suppressed when escaping from the lattices under the effective intensity modulator. As a result, the equidistant clusters can be rapidly formed. Besides, as there is no Kelly sideband in the pulse spectrum, and background pulses (more than 1000) are randomly distributed, the pulse interaction through DW and GDR can be neglected. What we should emphasize is that the self-organization dynamics process here is different from the HML buildup process. The buildup of HML undergoes a long-term pulse separating process under the combined effects of DW, acoustic wave and GDR.[6] However, the buildup of the equidistant clusters undergoes a rapid selective amplifying and self-organizing buildup process, which is dominated by the strong optomechanical effect. To the best of our knowledge, this is the first experimental observation of TR_{21} acoustic response-dominated birth dynamics of multipulse operation. This kind of birth dynamics is unlikely to be observed under the effect of R_{0m} acoustic response or in all-single-mode-fiber laser as the optomechanical effect is weak.

Despite the complex dynamics of the pulses inside the cluster, the cluster is stable in the energy and the temporal position. The equidistant nature of the clusters can coherently drive the acoustic waves to form the acoustic resonance. It should be noted that the optomechanical effect induces both the repulsive force and attractive force to mediate the long-range pulse interaction. Under the acoustic resonance, the optomechanical lattices can form the trapping potential to stabilize the HML. This leads to the fact that the quasi-stable equidistant clusters are mediated by both the trapping potential and intensity modulation under the effect of the TR_{21} acoustic resonance.

4. Conclusions and perspectives

In this work, we report a novel organized multipulse pattern with an interesting selectively amplifying self-organiziing buildup process under strong TR_{21}-induced optomechanical effect in microfiber-assisted ultrafast fiber laser. The organized multipulse pattern has good self-starting capability, repeatability, short buildup duration (less than 3 ms), and HML-like behavior. The results can deepen the understating of dynamics of pulses as well as the optoacoustic interaction, and exhibit a new way of achieving optomechanically controlled ultrafast fiber laser. Besides, the demonstrated ordered multipulse pattern has potential applications in advanced information processing, *etc*.

References

[1] Ryczkowski P, Närhi M, Billet C, Merolla J M, Genty G and Dudley J M 2018 *Nat. Photon.* **12** 221
[2] Grelu P and Akhmediev N 2012 *Nat. Photon.* **6** 84
[3] Liu X, Yao X and Cui Y 2018 *Phys. Rev. Lett.* **121** 023905
[4] Wang Z Q, Nithyanandan K, Coillet A, Tchofo-Dinda P and Grelu P 2019 *Nat. Commun.* **10** 830
[5] He W, Pang M, Yeh D H, Huang J, Menyuk C R and Russell P S J 2019 *Nat. Commun.* **10** 5756
[6] Liu X and Pang M 2019 *Laser Photon. Rev.* **13** 1800333
[7] Wang X, Peng J, Huang K, Yan M and Zeng H 2019 *Opt. Express* **27** 28808
[8] Sulimany K, Lib O, Masri G, Klein A, Fridman M, Grelu P, Gat O and Steinberg H 2018 *Phys. Rev. Lett.* **121** 133902
[9] Chouli S and Grelu P 2010 *Phys. Rev. A* **81** 063829
[10] Herink G, Kurtz F, Jalali B, Solli D R and Ropers C 2017 *Science* **356** 50
[11] Tang D Y, Zhao B, Zhao L M and Tam H Y 2005 *Phys. Rev. E* **72** 016616
[12] Grudinin A B and Gray S 1997 *J. Opt. Soc. Am. B* **14** 144
[13] Kutz J N, Collings B, Bergman K and Knox W 1998 *IEEE J. Quantum Electron.* **34** 1749
[14] Korobko D A, Okhotnikov O G and Zolotovskii I O 2015 *Opt. Lett.* **40** 2862
[15] Pang M, He W, Jiang X and Russell P S J 2016 *Nat. Photon.* **10** 454
[16] Jang J K, Erkintalo M, Murdoch S G and Coen S 2013 *Nat. Photon.* **7** 657
[17] Weill R, Bekker A, Smulakovsky V, Fischer B and Gat O 2016 *Optica* **3** 189
[18] Pilipetskii A N, Golovchenko E A and Menyuk C R 1995 *Opt. Lett.* **20** 907
[19] Wang Z, Wang Z, Liu Y, He R, Zhao J, Wang G and Yang G 2018 *Opt. Lett.* **43** 478
[20] Pang M, Jiang X, He W, Wong G K L, Onishchukov G, Joly N Y, Ahmed G, Menyuk C R and Russell P S J 2015 *Optica* **2** 339
[21] Kang M S, Brenn A, Wiederhecker G S and Russell P S J 2008 *Appl. Phys. Lett.* **93** 131110
[22] Kang M S, Nazarkin A, Brenn A and Russell P S J 2009 *Nat. Phys.* **5** 276
[23] He W, Pang M, Yeh D H, Huang J and Russell P S J 2021 *Light Sci. Appl.* **10** 1
[24] Shelby R M, Levenson M D and Bayer P W 1985 *Phys. Rev. B* **31** 5244
[25] Jarschel P F, Magalhaes L S, Aldaya I, Florez O and Dainese P 2018 *Opt. Lett.* **43** 995
[26] Lee K S, Ha C K, Moon K J, Han D S and Kang M S 2019 *Commun. Phys.* **2** 141
[27] Kbashi H J, Sergeyev S V, Al-Araimi M, Rozhin A, Korobko D and Fotiadi A 2019 *Opt. Lett.* **44** 5112
[28] Huang L, Zhang Y, Cui Y, Qiu J and Liu X 2020 *Opt. Lett.* **45** 4678
[29] Zhang R L, Wang J, Liao M S, Li X, Guan P W, Liu Y Y, Zhou Y, Gao W Q 2019 *Chin. Phys. B* **28** 034203
[30] Zhang R L, Wang J, Zhang X Y, Lin J T, Li X, Kuan P W, Zhou Y, Liao M S and Gao W Q 2019 *Chin. Phys. B* **28** 014201
[31] Cao M, Li H, Tang M, Mi Y, Huang L and Ren G 2019 *J. Opt. Soc. Am. B* **36** 2079
[32] Svelto O and Hanna D C 2010 *Principles of lasers*, 5th edn. (New York: Springer) pp. 313–319
[33] Liu X and Cui Y 2019 *Adv. Photon.* **1** 016003
[34] Liu X, Popa D and Akhmediev N 2019 *Phys. Rev. Lett.* **123** 093901
[35] Dianov E M, Luchnikov A V, Pilipetskii A N and Prokhorov A M 1992 *Appl. Phys. B* **54** 175
[36] Yeh D H, He W, Pang M, Jiang X, Wong G and Russell P S J 2019 *Opt. Lett.* **44** 1580